# Optimization of kinetostatic performances and compactness of an in vivo serial robot for minimally invasive surgery

Christophe Drouin, Sylvain Miossec, Carl A. Nelson, Gérard Poisson

▶ **To cite this version:**

Christophe Drouin, Sylvain Miossec, Carl A. Nelson, Gérard Poisson. Optimization of kinetostatic performances and compactness of an in vivo serial robot for minimally invasive surgery. 21ème Congres Français de Mécanique, Aug 2013, Bordeaux, France. hal-00836776v1

**HAL Id: hal-00836776**

**https://hal.science/hal-00836776v1**

Submitted on 24 Jun 2013 (v1), last revised 24 Jun 2013 (v2)

**HAL** is a multi-disciplinary open access archive for the deposit and dissemination of scientific research documents, whether they are published or not. The documents may come from teaching and research institutions in France or abroad, or from public or private research centers.

L'archive ouverte pluridisciplinaire **HAL**, est destinée au dépôt et à la diffusion de documents scientifiques de niveau recherche, publiés ou non, émanant des établissements d'enseignement et de recherche français ou étrangers, des laboratoires publics ou privés.

# Optimization of kinetostatic performances and compactness of an *in vivo* serial robot for minimally invasive surgery

C. Drouin[a], S. Miossec[a], C.A. Nelson[b], G. Poisson[a]

a. *University of Orleans, PRISME Laboratory, Bourges, Centre, FRANCE*
b. *University of Nebraska-Lincoln, Mechanical and Materials Engineering, Lincoln, NE, USA*

## Résumé :

*Dans cet article, nous optimisons les dimensions des corps d'un robot de chirurgie mini-invasive muni de deux bras sériels pour améliorer ses performances cinétostatiques (force, vitesse) ainsi que sa compacité, sous contraintes d'espace atteignable. Une courbe de Pareto est tracée pour fournir au concepteur toutes les solutions optimales possibles entre les vitesses, les forces transmises ainsi que la compacité.*

## Abstract :

*In this paper, we optimize the link dimensions of a robot with two serial arms for minimally-invasive surgery, to improve its kinetostatic performance (force, velocity) and its compactness, under the constraint of reachable space. A Pareto curve is plotted to provide the designer all the optimum possible solutions between transmissible velocity, forces, and compactness.*

**Mots clefs : medical robots ; optimal design ; multiobjective optimization ; dimensional synthesis**

## 1 Introduction

The medical application of minimally invasive surgery (MIS) is a different technique compared to open surgery, which consists of operating on the patient through trocars (ports placed to stabilize small incisions) to reduce operative trauma stress. Laparoendoscopic single-site surgery (LESS) is another technique based on MIS : the surgeon passes his instruments through a single trocar instead of multiple ones. The complexity of the movements required in these techniques highlights the utility of robotic systems to help the surgeon in his gestures. For LESS purposes, the *in vivo* robots have the advantage of being compact in nature, but their design is challenging to simultaneously avoid collisions, seek for the best compactness and get the best transmissible velocity and force at the end-effector (kinetostatic performance). At the University of Nebraska-Lincoln, several robots have been developed and tested [2, 5, 9, 11]. Workspace, kinetostatic performance and simplicity of insertion were the major points of development and evolution of these robots. Many compromises in the design need to be made, difficult to solve with only a CAD approach. In this paper, we present the dimensional synthesis of such an *in vivo* robot, mathematically formulated, to improve simultaneously its compactness and its kinetostatic performance, while taking into account workspace constraints. The robot has a 2R-R-R architecture (Figure 1) and is a two-armed serial robot, designed for LESS surgery operations.

## 2 Robot overview

### 2.1 Robot structure

The robot kinematic architecture and its Denavit-Hartenberg parameters [7] are presented in Figure 2 and Table 1, with $j = 1..2$, corresponding to the right and left arm.

**FIGURE 1** – Robot structure

| Joint | 1 | 2 | 3 | 4 |
|---|---|---|---|---|
| $\alpha_{i-1j}$ | $(-1)^{j+1}\frac{\pi}{2}$ | $(-1)^{j+1}\frac{-\pi}{2}$ | 0 | $\frac{-\pi}{2}$ |
| $a_{i-1j}$ | 0 | 0 | $a_{2j} = L_{2j}$ | 0 |
| $\theta_{ij}$ | $\theta_{1j}$ | $\theta_{2j}$ | $\theta_{3j}$ | $\theta_{4j}$ |
| $r_{ij}$ | $r_{1j} = L_{1j}$ | 0 | 0 | $r_{4j} =$ |
| $\theta$ (fig. 2) | $\delta\theta_{11}$ | 0 | $\frac{-\pi}{2} + \delta\theta_{31}$ | $\frac{-\pi}{2}$ |
| V (rad/s) | 0.97 | 1.11 | 1.11 | / |
| T (Nmm) | 1220.61 | 264.17 | 264.17 | / |

**TABLE 1** – Denavit-Hartenberg parameters

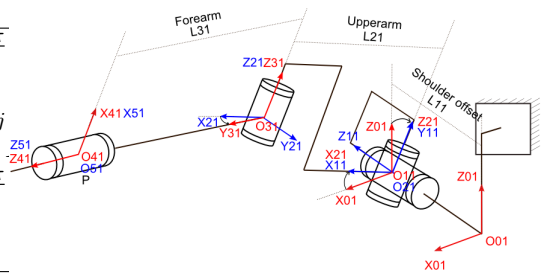


**FIGURE 2** – Kinematic architecture (right arm)

$L_{11}$ defines the shoulder offset equal to 17.5 mm while $L_{21}$ and $L_{31}$ are the parameters to optimize.

## 2.2 Direct and inverse model

The direct model is the expression of the end effector position in operational space, function of joint motions, as written below :

$$\begin{pmatrix} PX_j \\ PY_j \\ PZ_j \end{pmatrix} = f(\begin{pmatrix} \theta_{1j} \\ \theta_{2j} \\ \theta_{3j} \end{pmatrix}) \tag{1}$$

For the right arm, we will have :

$$\begin{pmatrix} PX_1 \\ PY_1 \\ PZ_1 \end{pmatrix} = \begin{pmatrix} c_{\theta_{11}}(c_{\theta_{21}}(L_{21} - L_{31}s_{\theta_{31}}) - L_{31}s_{\theta_{21}}c_{\theta_{31}}) \\ s_{\theta_{21}}(L_{21} - L_{31}s_{\theta_{31}}) + L_{31}c_{\theta_{21}}c_{\theta_{31}} - L_{11} \\ s_{\theta_{11}}(c_{\theta_{21}}(L_{21} - L_{31}s_{\theta_{31}}) - L_{31}s_{\theta_{21}}c_{\theta_{31}}) \end{pmatrix} \tag{2}$$

and the equations of the inverse model are :

$$\begin{pmatrix} \theta_{11} \\ \theta_{21} \\ \theta_{31} \end{pmatrix} = \begin{pmatrix} atan2(PZ_1, PX_1) \\ atan2(\alpha(L_{11} - \gamma\ L_{21}) - \beta\ \lambda\ L_{21}, \alpha\ L_{21}\ \lambda + \beta(L_{11} - L_{21}\ \gamma)) \\ atan2((L_{21}^2 - \alpha^2 - \beta^2 + L_{11}^2)/(2L_{11}), \pm\sqrt{\alpha^2 + \beta^2 - L_{11}^2 + 2\gamma\ L_{11}L_{21} - \gamma^2 L_{21}^2}) \end{pmatrix} \tag{3}$$

with :

$$\alpha = PZ_1 - L_{11},\ \beta = -PZ_1 s_{\theta_{11}} - PX_1 c_{\theta_{11}} \tag{4}$$

$$\gamma = s_{\theta_{31}},\ \lambda = c_{\theta_{31}} \tag{5}$$

The study of the inverse model shows there is no solution in two different cases, corresponding to the unreachable positions of the robot as described in the following section.

## 2.3 Jacobian and singularities

The direct instantaneous kinematic model gives the relation between the joint angular velocities and the end-effector velocities :

$$\dot{X}_j = J_j \dot{Q}_j,\ Q_j = [\theta_{1j}\ \theta_{2j}\ \theta_{3j}]^T \tag{6}$$

With $J_1$ detailed as follow :

$$J_1(1) = \begin{pmatrix} L_{31}s_{\theta_{11}}(s_{\theta_{31}+\theta_{21}} - L_21c_{\theta_{21}}) \\ 0 \\ -L_{31}c_{\theta_{11}}(c_{\theta_{21}+\theta_{31}} + L_{21}c_{\theta_{21}}) \end{pmatrix} \tag{7}$$

$$J_1(2) = \begin{pmatrix} -L_{31}c_{\theta_{11}}(c_{\theta_{31}-\theta_{21}} - L_21s_{\theta_{21}}) \\ -L_{31}(c_{\theta_{21}+\theta_{31}} + L_21c_{\theta_{21}}) \\ -L_{31}s_{\theta_{11}}(c_{\theta_{31}-\theta_{21}} + L_21s_{\theta_{21}}) \end{pmatrix} \tag{8}$$

$$J_1(3) = \begin{pmatrix} -L_{31}c_{\theta_{11}}c_{\theta_{21}+\theta_{31}} \\ -L_{31}c_{\theta_{21}+\theta_{31}} \\ -L_{31}s_{\theta_{11}}c_{\theta_{21}+\theta_{31}} \end{pmatrix} \tag{9}$$

The study of these three vectors shows that three cases of singularities can occur ; in particular, a singularity appears when the forearm and upper arm are aligned or bent over backwards ; this indicates the exterior and interior boundaries of the workspace, giving a hollow sphere (Figure 3). Another case shows there are two unreachable lines in this sphere, forming two lines as indicated in Figure 3 in sandy-brown. Other voids depend on motion limits of the joints and on collisions of the robot mechanical parts, which are not considered in this paper.

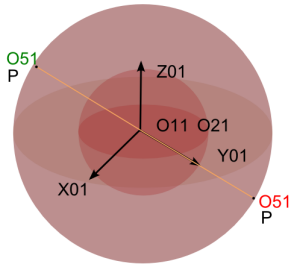


**Figure 3** – Robot workspace

# 3 Optimization

## 3.1 Data

The shape formed by the desired reachable tool-positions is approximated by an ellipsoid whose semi-major and semi-minor axes are determined based on the minimal and maximal bounds of some data presented in [9]. These data are based on two operations (open cholecystectomy and colectomy), performed on a porcine model. The two data sets give two ellipsoids for the two arms.

## 3.2 Constraints

Considering the fact that the robot-arm workspace is a hollow sphere, the two ellipsoids must be inside the reachable positions of their spheres. Assuming that $L_{3j} < L_{2j}$, we must have $L_{2j} - L_{3j} < min(D_{S_j})$ and $L_{2j} + L_{3j} > max(D_{S_j})$, with $D_{Sj}$ the set of distances from $O_{1j}$ to a desirable position $M_{nj}$. These two workspace constraints will be written as $C_{W_{1j}}$ and $C_{W_{2j}}$.
The second type of constraint concerns the collisions that may occur between the two arms during an operation : they can be avoided if $\theta_{11} \in [-180^\circ ; 0^\circ]$ and $\theta_{12} \in [0^\circ ; 180^\circ]$, meaning that two different solutions to the inverse model of the two arms must be considered.

## 3.3 Performance criteria

Based on Briot's work [1], we maximize the coefficients $\min_{S_j}(k_{Vij}^{min})$ and $\min_{S_j}(k_{Fij}^{min})$, calculated as the lowest values of transmission factors in velocity and forces on the sets $S_j$, with $S_j$ the two tool-tip position sets, $S_j = \{M_{1j}; M_{2j}...; M_{nj}\}$. These two coefficients define the two kinetostatic performance criteria

$P_{Velocity}$ and $P_{Force}$ to maximize, written as follows : $P_{Velocity_j} = \underset{S_j}{min}(k_{Vij}^{min})$ and $P_{Force_j} = \underset{S_j}{min}(k_{Fij}^{min})$.
The $k_{Vij}^{min}$ factor represents the minimal transmission factor in velocity, in one direction at the end effector, for a given point $M_{ij}$. This factor will be zero when we reach a singularity. We have : $k_{Vij}^{min} = min_j(k_{ghl}^m) = \sqrt{J_{2j}^T J_{2j} - (J_{2j}^T J_{1j})(J_{1j}^T J_{1j})^{-1}(J_{1j}^T J_{2j})}$, where $J_{2j} = [I_{gj}\ I_{hj}]$, $J_{1j} = (-1)^m I_{lj}$, for $g, h, l = 1, 2, 3$, $g \neq h \neq l$, $m = 1$ or 2, with $[I_{1j}\ I_{2j}\ I_{3j}] = J_j\ diag(\dot{\theta}_{kjmax})$. $\dot{\theta}_{kjmax}$ represents the maximal velocity of the $k^{th}$ actuator of the $j^{th}$ arm. We also have $k_{Vj}^{max} = max_l(\|J_j(q)e_l\|)$, for l=1 to 4, with $e_1 = [1; -1; 1]^T$ $e_2 = [1; 1; 1]^T$ $e_3 = [1; 1; -1]^T$ $e_4 = [1; -1; -1]^T$. The same evaluation of $(k_{Fij}^{min})_{S_j}$ is done by replacing $J_j\ diag(\dot{\theta}_{kjmax})$ with $J_j^{-T}\ diag(T_{kjmax})$ , where $T_{kjmax}$ represents the maximal torque of the $k^{th}$ actuator of the $j^{th}$ arm. As for $k_{Vij}^{min}$, $k_{Fij}^{min}$ represents the minimal transmission factors in force for a given point $S_j$. It is the smallest transmissible force by the robot in the worst direction on the end effector. This factor can be calculated through a statical equilibrium.
Compared to some indices like the dexterity [3] or the manipulability [12], the indices presented by Briot are more adapted. Indeed, if performance is related to precision, isotropy or the identification of singularities, they are well adapted but they do not take into account the heterogeneity of the actuators since they consider the norm of the input velocities equal to one, which is not the physical reality [8]. This heterogeneity is the main difference compared to the two factors.
Taking into account the actuators characteristics will give another ideas of the performances for any point of the workspace. In particular, it will be different near a singularity since we could have $\sigma_{min} \neq k_{Vij}^{min}$. And the global conditioning index [4] will not be representative of the global kinetostatic performances of the robot. Another difference concerns the fact the dexterity or the manipulability gives values between $[0; 1]$, which are not relevant to say what number correspond to good performances. Here, the $k_{Vij}^{min}$ and $k_{Fij}^{min}$ give the real values of minimal velocity and force. Finally, the dexterity and manipulability are the aggregation of the two factors, and it is not then possible to distinguish the parallel from serial singularities.
For all these reasons, the indices presented by Briot and called minimal transmission factor in velocity or force, are more appropriate.
The last criterion to optimize in the problem is the compactness ; this criterion has been simply defined as the sum of lengths $L_{2j}$ and $L_{3j}$, as follows : $P_{Compactness_j} = \frac{(L_{2j}+L_{3j})}{2}$

## 3.4 The objective function

A gradient-based method was used to find the optimal parameters satisfying the constraints and giving the optimal solutions between compactness and kinetostatic performances. The problem was formulated as follows : $min\ f(X)_j = \beta[(1-\alpha)(P_{Compactness_j}) + \alpha N(P_{Velocity_j})] + (1-\beta)(P_{Force_j})$, $subject\ to$ $C_{W_kj}(V) > 0$, $k = 1...2$ with N a normalization coefficient, $\alpha$ and $\beta$ two weighting coefficients between the three criteria, $\alpha, \beta = [0; 1]$ to compute the Pareto curve as explained below.

## 3.5 Results and Comparison with another architecture

Results of optimization are presented in Figures 4, 5 and 6 for the left arm : results and interpretations of the right one are similar. ($P_{Velocity}$ is in mm/s and $P_{Force}$ is in N). Each point is an optimal solution $(L_{2j}, L_{3j})$, obtained by varying $\alpha$ and $\beta$. One can see the the compact solution figure 6 in $XZ$ plan, and the same solution in $XY$ plan figure 5.

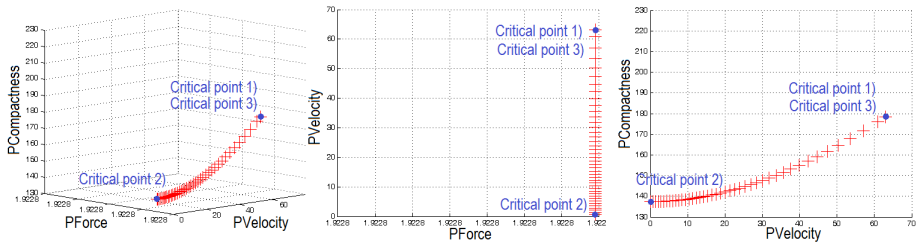


**Figure 4** – Pareto curves for the left arm ($P_{Velocity}$ in mm/s, $P_{Force}$ in N and $P_{Compactness}$ in mm).

We define the three critical points as 1) the maximum of $P_{Compactness}$, 2) the minimum of $P_{Velocity}$ and 3) the compromise between $P_{Velocity}$ and $P_{Compactness}$. For the last one, we define the compromise between compactness and velocity as the opposite relative variations [10] ; we would have $dP_{Compactness}/P_{Compactness} = -P_{Velocity}/P_{Velocity}$ ; with this definition, for a small variation along the Pareto front that will improve one criterion by 1%, it will degrade the other criterion by 1%.

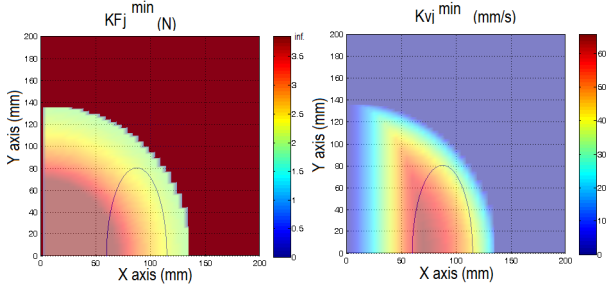


**FIGURE 5** – Evolution of $k_{Vj}^{min}$ (in mm/s) and $k_{Fj}^{min}$ (in N) for point 2) in $ZX$ plan

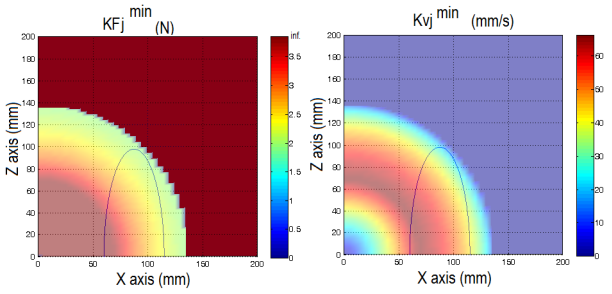


**FIGURE 6** – Evolution of $k_{Vj}^{min}$ (in mm/s) and $k_{Fj}^{min}$ (in N) for point 2) in $XY$ plan

Results of optimization for the left arm are indicated below :
$(L_{2j}; L_{3j}) = (68.69; 68.69), P_{Compactness} = 137.38, P_{Velocity} = 0.009, P_{Force} = 1.92$ (point 2)).
$(L_{2j}; L_{3j}) = (89.13; 89.13), P_{Compactness} = 178.27, P_{Velocity} = 63.05, P_{Force} = 1.92$ (point 1) and 3)).

The study of these figures show first point 3) is mingled with point 1). It means that from a mechanical point of view, it is unprofitable to improve the compactness since it highly reduces the velocity. Secondly, we see $P_{Force}$ is constant for any couple $(L_{21}; L_{31})$. To explain that, we recall $P_{Force}$ represents the lowest values of the minimal transmissible forces for a given couple $(L_{21}; L_{31})$, for any configurations associated to the set $S_1$. Let's then consider a force applied at the end effector ; the statical equilibrium of the robot indicates the smallest compensated force always depends on the 2nd joint, calculated as the ratio between the maximal torque $T_{21} = 264.17\ Nmm$ and the distance from $O_{11}$ to the farther point of the ellipsoid ($d_{max} = 137\ mm$). The result is constant since this distance is constant. Thirdly, the results show it is useless to increase the link lengths when $P_{Velocity}$ reaches a limit at 63.05 $mm/s$, point 3) : starting from this point, when $L_{21}$ and $L_{31}$ increase, the smallest velocity contribution in the workspace depends only on the 1st joint and is equal to the product between $V_{11\ max} = 0.97\ rad/s$ with the distance from $O_{11}$ to the closest point of the ellipsoid in $ZX$ plane ($d_{min_{zx}} = 65\ mm$).
These results indicate the minimal transmissible force depends only on the 2nd joint ; ideally, it would have depend on the three joints and not only one to equilibrate : the 2nd link is under-dimensioned. Moreover, from point 2) to 3), $P_{Velocity}$ depends on the 2nd and 3rd joints characteristics and the links lengths increasing ; but from point 3), increasing the lengths is useless since $P_{Velocity}$ does not depend on the robot configuration but only on the 1st joint characteristic. More precisely, it depends only on $V_{21\ max}$ and $d_{min_{zx}}$. Moreover, we see the minimal transmissible velocity is dependent on the 2nd and 3rd joint, near singular configurations. Then for a certain couple $(L_{21}; L_{31})$, it is useless to increase the link lengths to improve $P_{Velocity}$, since it depends only on the 1st link : its minimal velocity does not depend on the robot configuration, but on $V_{21\ max}$ and $d_{min_{zx}}$.

Such a dimensional synthesis was previously performed for the same purposes, but with another architecture [6]. The two first joint were interchanged, giving another workspace. The actuators characteristics were also different, giving other kinetostatic performances. Results of optimization for the left arm with this architecture are indicated below :
$(L_{2j}; L_{3j}) = (101.29; 36.10), P_{Compactness} = 137.39, P_{Velocity} = 0.64, P_{Force} = 6.80$ (point 2))
$(L_{2j}; L_{3j}) = (111.12; 63.51), P_{Compactness} = 174.64, P_{Velocity} = 85.25, P_{Force} = 3.87$ (point 1) and 3)).

This robot has been designed taking into account highest integration constraint than for the other one. It is interesting to note the kinetostatic performances are better for this robot than the one presented in this paper, though we would have expected the opposite. This is due to technological choice (less powerful motor) and it indicates the kinetostatic performances of our robot could be largely bet-

ter, with an appropriate choice of actuators and gear ratios. Moreover, compared to the other one, our robot workspace is less problematic : the sequence of the 1st and 2nd link is different and creates some spherical voids in the workspace, while we only have lines here. This is relevant since the topology constrains the size and shape of data. The differences between these two version of *in vivo* robots is due to the insertion procedure : for our robot, each arm is passed through the trocar, while the other one can be entirely deployed inside the peritoneal cavity. Results of optimization for each robot show the need to couple simultaneously the dimensional synthesis, the choice and integration of actuators : it is indeed necessary to equilibrate the power in velocity and force of each actuators.

# 4 Conclusion

The dimensional synthesis of a two-arm robot with 2R-R-R architecture has been presented in this paper, for MIS surgery. The link dimensions have been optimized to give the designer the solutions balancing the minimum transmissible velocity, force and compactness, under constraints of workspace, taking into account the actuator characteristics. The results show the under-dimensioning of some actuators ; in particular, it would be interesting to re-dimension the actuators of the 2nd joint and the 1st one to improve the kinetostatic performances. A brief comparison with another 2R-R-R architecture highlights the need to couple simultaneously the dimensional synthesis with the choice of actuators. Our future work will concern the re-dimensioning of the actuators for this robot. Ideally, the dimensional synthesis could be coupled with the integration of actuators, which could be done under workspace constraint, more realistic collisions constraints, but also some insertion and integration constraints.

# Références

[1] Briot S. Pashkevich A. and Chablat D. Optimal technology-oriented design of parallel robots for high-speed machining applications. *International Conference on Robotics and Automation*, 2010.

[2] Pourghodrat A. Nelson C. A. and Midday J. Pneumatic miniature robot for laparoendoscopic single incision surgery. *International Design Engineering Technical Conference*, 2011.

[3] Gosselin C. and Angeles J. The optimum design of a spherical three-degree-of-freedom parallel manipulator. *Journal of Mechanisms, Transmissions, and Automation in Design*, 111, No 2 :202–207, 1989.

[4] Gosselin C. and Angeles J. A global performance index for the kinematic optimization of robotic manipulators. *Journal of Mechanism Design*, 1991.

[5] Piccigallo M. Scarfogliero U. Quaglia C. and Petroni G. Design of a novel bimanual robotic system for single-port laparoscopy. *Transactions on Mechatronics*, 2010.

[6] Drouin C. Pourghodrat A. Miossec S. Poisson G. and Nelson C. A. Dimensional optimization of a two-arm serial robot for single-site surgery operations. *International Design Engineering Technical Conference*, 2013.

[7] Denavit J. and Hartenberg R. A kinematic notation for lower-pair mechanisms based on matrices. *Journal of Applied Mechanics*, 1955.

[8] Merlet J.P. Jacobian, manipulability, condition number, and accuracy of parallel robots. *Journal of Mechanical Design*, 2006.

[9] Wortman T. D. Strabala K. W. Lehman A. C. Farritor S. M. and Oleynikov D. Laparoendoscopic single-site surgery using a multi-functional miniature in vivo robot. *International Journal of Medical Robotics and Computer Assisted Surgery*, 2011.

[10] S. Miossec and L. Nouaille. Structural link optimization of an echography robot. *IFToMM*, 2011.

[11] Lehman A.C. Wood N.A. Farritor S. Goede M.R. and Oleynikov D. Dexterous miniature robot for adavanced minimally invasive surgery. *Surgical Endoscopy*, 2011.

[12] Yoshikawa T. Manipulability of robotic mechanisms. *Intenational Journal of Robotics Research*, 1985.